Article

A Low-Cost Continuous Turbidity Monitor

David Gillett [1] and Alan Marchiori [2]*

[1] Department of Chemical Engineering, Bucknell University; dog003@bucknell.edu
[2] Department of Computer Science, Bucknell University; amm042@bucknell.edu
* Correspondence: amm042@bucknell.edu; Tel.: +1-570-577-1751

Academic Editor: name
Version May 24, 2019 submitted to Sensors

Abstract: Turbidity describes the cloudiness, or clarity, of a liquid. It is a principle indicator of water quality, sensitive to any suspended solids present. Prior work has identified low-cost turbidity monitoring as a significant hurdle to overcome to improve water quality in many domains, especially in the developing world. Low-cost hand-held benchtop meters have been proposed. This work adapts and verifies the technology for continuous monitoring. Lab tests show the low-cost continuous monitor can achieve the 0.1 NTU accuracy desired for water quality monitoring. A thirty-eight day continuous monitoring trial, including in steady state conditions and the response to a step change in turbidity, showed promising results with median error of 0.0574 NTU for one sensor. However, noise was present in the readings. The cause was primarily attributed to ambient light and bubbles in the water. By controlling these error sources, we believe the low-cost continuous turbidity monitor could be a useful tool for water quality management in multiple domains.

Keywords: turbidity; low-cost; continuous water quality monitor; water;

---

1. Introduction

The United Nations states that water is at the core of sustainable development and is critical for socioeconomic development, healthy ecosystems, and for human survival itself. It is vital for reducing the global burden of disease and improving the health, welfare, and productivity of human populations. It is central to the production and preservation of a host of benefits and services for people. Water is also at the heart of adaptation to climate change, serving as the crucial link between the climate system, human society, and the environment [1].

Water quality monitoring is the process by which critical characteristics of water (physical, chemical, biological) are measured. Turbidity is one of the most universal metrics of water quality. It is a measure of the cloudiness (the inverse of clarity) of water. In watersheds, the presence of high turbidity can be indicative of both organic and inorganic materials. In the case of organic materials, high turbidity can indicate problems such as increased algae growth caused by fertilizer run-off. In the case of inorganic materials, high turbidity can indicate problems such as high suspended sediment caused by erosion during a rainstorm or water churn caused by high winds. Turbidity is a non-specific measure and therefore alone cannot identify the root cause of water cloudiness. However, under certain conditions, it can be used to estimate certain quantitative parameters such as stream loading, total suspended solids, and soil loss. There is a variety of published research on the effect of turbidity on different organisms and the implications on human drinking water.

Therefore, turbidity is a useful measure for many water resource management applications. This monitoring can help inform decisions regarding the allocation of funds and what future actions would be the best for a watershed. Presently, the sensors that are used are expensive, typically costing thousands of dollars. This causes most of the sensors to be owned by companies that communities hire to take samples a small number of times a year. This is far from the best approach. The key to efficient and proactive water resource management is continuous and accurate monitoring. However, the cost and complexity of deploying such monitoring systems presently limit their use. It is critical that the cost of individual sensors be decreased to make widespread implementations of these monitoring systems feasible. Also, it is critical that the accuracy of these sensors be high enough to provide useful water quality data. Automated continuous sensing would allow the labor cost of water monitoring to decrease substantially as after the initial setup, with the exception of minor ongoing maintenance, the sensors run continuously without human intervention. An automated sensor platform could also be used by people with little, if any, formal training in water monitoring.

Open-source technologies have been identified as the most promising solution to this challenge [2]. As a result, some groups have begun developing their own low-cost monitoring solutions [3–5]. However, these prior works for turbidity monitoring focus on hand-held meters and leave continuous monitoring for future work. Lambrou et al. [6] builds a complete continuous monitoring system using off-the-shelf sensors without addressing cost or complexity concerns. In this paper, we present the development of a low-cost continuous turbidity sensor. Our goal is a sensor that could be used in both watershed and drinking water continuous monitoring applications.

2. Related Work

Standard laboratory methods to measure turbidity are well understood and the most commonly used standard is maintained as method 180.1 by the U.S. EPA [7]. This method specifies a tungsten lamp illuminating a sample from not more than 10 cm away with a photo-electric detector oriented 90° from the source. This method is specified from 0-40 nephelometric turbidity units (NTU) with instrument sensitivity of at least 0.02 NTU in water under 1.0 NTU. The NTU units themselves are defined by the response of the nephelometric sensor to known standards. There is no mathematical definition of NTU.

There are at least four other standards for measuring turbidity using nephelometry (ISO 7027, GLI Method 2, Hatch Method 101033, and Standard Methods 2130B) [8]. These variants specify different light sources and detector arrangements. However, none of these standard methods lend themselves to low-cost continuous water quality monitoring. In this work, we follow the general approach of using a light source with a detector located at 90° built using only commonly available electronic components, 3D printable structures, and open-source software with the goal of determining if such a low-cost sensor could be suitable for continuous water quality monitoring applications.

The current state of the art in the design of low-cost turbidity sensors is a sensor created by Christopher Kelly and his team [5]. To our knowledge, this project represents the first publicly available peer-reviewed characterization of an affordable nephelometric turbidimeter. The team set out to create a battery-powered, high accuracy turbidity meter for drinking water monitoring in low-resource communities. This goal required a few design constraints that they set out to meet: run on a single set of batteries for weeks to months of regular use, a high measurement accuracy and the ability to differentiate small changes in turbidity especially over the range of 0-10 NTU, the sensor must have all of its parts documented and be able to be made by non-experts who want to create their own version of the sensor.

The developed system is a cuvette-based turbidity meter using a single near infrared light emitting diode and a TSL230R light-to-frequency sensor set at 90° apart in a single beam design. A single beam design is one where there are a single LED emitter and a single receiver perpendicular to the light beam

Figure 1. Amphenol TST-10 (left) and TSD-10 (right). TSW-10 is similar to the TSD-10 (not pictured) (images from Amphenol).

from the LED. The receiver converts light intensity to a signal that can be read by a microcontroller. The theory behind this design is that the clearer the solution, the more light that makes it straight through the solution. The more turbid the solution, the more light that is reflected perpendicular to the light beam. The meter does not store the data but rather displays it on a LED display for manual recording. Using turbidity standards created using cutting oil and water, the team tested a known turbidity meter next to the created turbidity sensor and measured the readings from both. This data was used to create four calibration curves (each for a different range) that are used to convert the light-to-frequency sensor output from the created turbidity meter to the turbidity reported by the commercial sensor.

The study showed the created turbidity meter had an accuracy within 3% of the commercial sensor or 0.3 NTU whichever is larger over the range of 0.02 NTU to 1100 NTU. They reported that in 8 trials results were within 0.01 NTU for the four turbidity standards under 0.5 NTU. These results support the notion that a low-cost turbidity meter is a possibility, however, more tests to evaluate and verify these results are needed. The proposed next steps as of when the paper was written were to account for thermal fluctuations affect on the turbidity of a solution, minimizing the light leakage into the sensor housing through the external casing, investigating the use of GSM data transmission, and investigating an inline immersible version of the turbidity meter.

3. Appliance Sensors

As a first step to the development of a low-cost continuous turbidity sensor, we evaluated existing commercial low-cost appliance turbidity sensors. These sensors are used in dishwasher and clothes washing machines typically to determine when the contents of the appliance are clean. It was hoped that they would be able to sufficiently determine differences in water clarity enough to provide useful data for water management applications. Three different turbidity sensors from Amphenol were tested (TST-10, TSD-10, and TSW-10) pictured in Figure 1. All models contain an LED emitter and a phototransistor oriented directly across (180°) from the LED. The output is proportional to the amount of light traveling through the sample and arriving at the phototransistor instead of to the measurement of the scattered light provided by a nephelometric meter. The primary difference between the various models is the mechanical enclosure. The TST-10 is a flow-through design while the TSD-10 is designed to be inserted into the water flow. Either of these could be adapted for continuous monitoring applications.

Each sensor was tested using the reference circuit specified in the datasheet shown in Figure 2 [9–11] and recording the voltage output of the sensor using an Arduino Mega's internal analog to digital converter.

The more light that is transmitted through the sample to the receiver the higher the output voltage. This higher voltage means the solution is more clear which is equivalent to saying that it has lower turbidity.

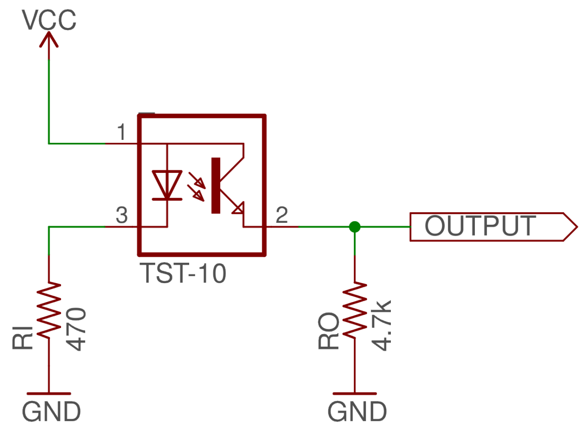

Figure 2. Amphenol (TST-10) appliance turbidity test circuit where VCC=5V. Other Amphenol models use the same circuit.

To test the hardware variation between sensors, we created test solutions by adding a small amount of cutting oil to water and tested two appliance sensors of the same model in the same solution. Ideally, both sensors should output the same voltage in the same solution. We performed a simple linear conversion from voltage to approximate NTU using the output curve specified in the data sheet for each sensor. Table 1 shows the observed variation between the sensors in this experiment. The result shows the actual variation is less than the worst-case value calculated from the curve in the data sheet. The TST-10 performed best with 50 NTU difference, however, for most water management applications this variation is far too large to be useful.

Table 1. Variation between two appliance sensors of the same model.

Sensor	Specified Variation (NTU)	Observed Variation (NTU)
TST-10	325	50
TSD-10	305	162
TSW-10	748	348

To improve accuracy we can individually calibrate each sensor. According to the TST-10 datasheet, the useful range of the sensor is $0 - 4000$ NTU with a voltage differential of 2.7 V. We used tap water (NTU$\approx$0) and recorded the sensor's maximum voltage. The minimum voltage is specified at 4000 NTU with output voltage 2.7 V less.

To estimate the sensor's precision we can use a first-order linear approximation of the output over the full 4000 NTU range of the sensor. Therefore, the maximum resolution of the sensor using the Arduino's 10-bit analog to digital converter is 7.25 NTU per ADC count. As the last bit of ADC output is typically noisy, we expect the best possible result using this approach to be $\pm$7.25 NTU with slightly better results under 1000 NTU and slightly worse results over 1000 NTU due to the non-linear output of the sensor. For most water management applications, $\pm$1 NTU is useful, therefore, we conclude that directly connecting the sensors to the ADC cannot provide the needed resolution for water management applications even without noise or other sources of error.

4. Validation of the low-cost nephelometric sensor

From our previous experiments with the appliance sensors and the Arduino's analog to digital converter (ADC), we conclude a nephelometric sensor with higher resolution ADC is necessary to achieve the precision necessary for water management applications. To explore this design space, we first constructed a sample-based sensor similar to the one developed by Kelley et al. [5].

This design overcomes the ADC precision by using a TAOS TSL235R light to frequency converter, shown in Figure 3, to measure light intensity rather than providing an analog output. Internally the device has a photodiode sensitive to light in the range 320 nm - 1050 nm. The diode current is converted to a square wave with 50% duty cycle where the output frequency is proportional to the light intensity. The range of frequencies that the converter outputs are from 0-800 kHz. Using the Arduino's onboard Timer/Counter and Paul Stoffregen's FreqCount library [12], we can measure the average frequency over a short interval (e.g., 100 ms) with very high accuracy and precision. This approach to measuring light intensity results in far greater resolution than what is possible using the Arduino's ADC. As a result, the sensor has a much larger dynamic range yielding higher resolution readings that are no longer strongly limited by the ADC resolution.

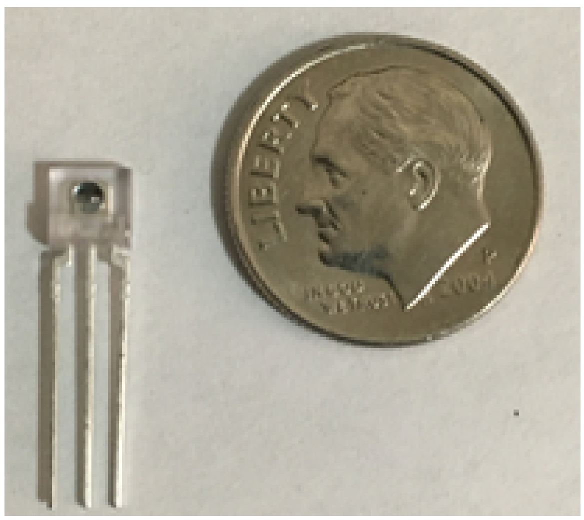

Figure 3. TAOS TSL235R light-to-frequency converter.

To evaluate the sensor, we constructed a simple test tube based design that was 3D printed shown in Figure 4. The test tube holder allowed the 100 mA IR LED and TAOS TSL234R to be mounted securely in both 90° and 180° configurations. The IR LED was driven by an Arduino GPIO pin through a series 1K Ohm resistor. The frequency count was read using are read using FreqCount on an Arduino Mega 2560.

Figure 5 shows the results from several validation tests of the light-to-frequency sensor. The Figure shows the average and the standard deviation of 10 measurements given on the X-axis. From these results, we can clearly identify empty test tubes and an empty test chamber (i.e., no test tube inserted). The results with 126 NTU calibration solution and distilled water show approximately 1329 Hz difference with < 3 Hz of standard deviation. A two-point calibration from these values suggests sensing resolution greater than 0.1 NTU per Hz is possible.

However, these results are promising but not as good as those reported by Kelly et al. We suspect some of the error is due to the large reflections and suspected optical impurities in the test tube. Because of the circular shape of the test tube, it is nearly impossible to keep the IR LED exactly perpendicular to its

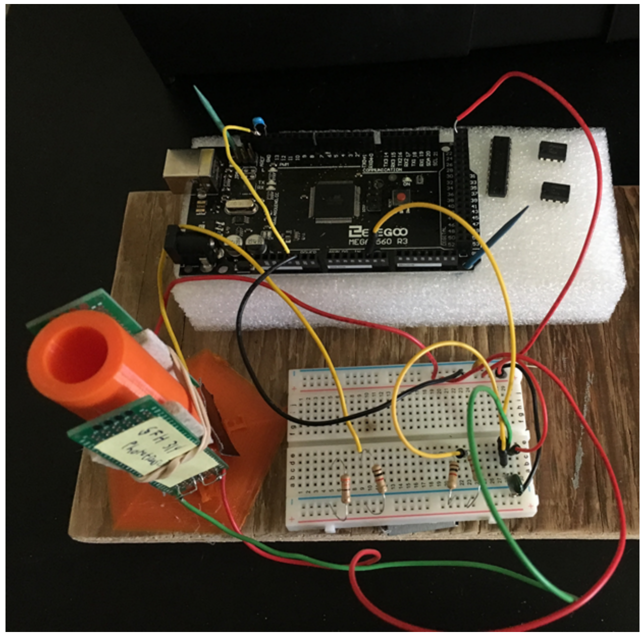

Figure 4. Circular sample holder and test circuit.

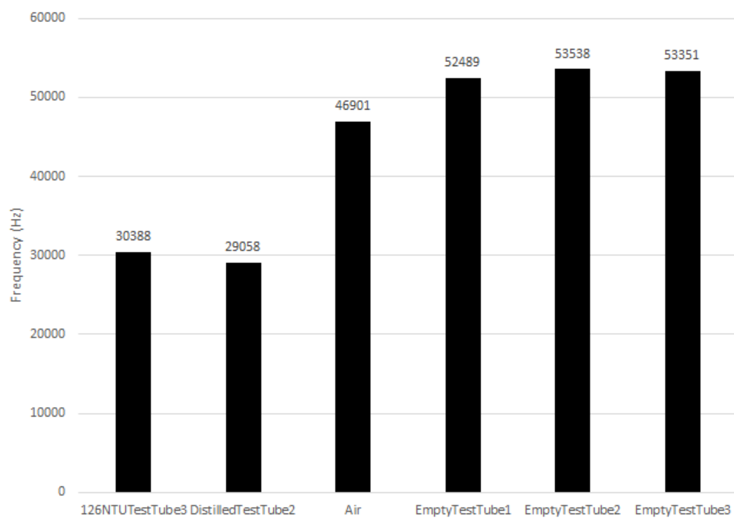

Figure 5. Light-to-frequency initial results using standard test tubes.

surface. As a result, we decided to switch to plastic cuvettes as used by Kelly et al. Cuvettes have straight sides and are typically used in spectrophotometry where optical clarity is important.

To accept the striated-sided cuvettes, the housing was redesigned to have a square shape with internal walls to block any light from getting to the receiver unless it first went through the sample as shown in Figure 6a. We tested the sample holder with distilled water and a calibration solution. The test solutions were measured with a calibrated Hach 2100P turbidity meter before the experiment and measured 0.39 and 86 NTU respectively. Figure 6b shows the observed frequency output from the light to frequency converter. This shows on average a 600 Hz difference, or about 7 Hz per NTU assuming a linear response.

However, there is some overlap in the measured results between the samples and this resolution is slightly worse than the test-tube based design.

After investigation, we found that the cuvettes could rotate slightly in the sample holder and that external ambient light was causing variation in the output frequency. To rectify these problems, we revised the design to have a tighter fit to the cuvette to eliminate rotation and increased the wall thickness to reduce the effect of external light. The revised sample holder is shown in Figure 6c. We repeated the experiment with distilled water and our calibration solution. The results in Figure 6d show a significant reduction in frequency at both readings and significantly reduced variation. This result is consistent with the reduction of external light and constant cuvette position. Although the average frequency difference was reduced to 360 Hz (4.2 Hz per NTU), the frequency noise was greatly reduced and both samples yield statistically different readings in all cases.

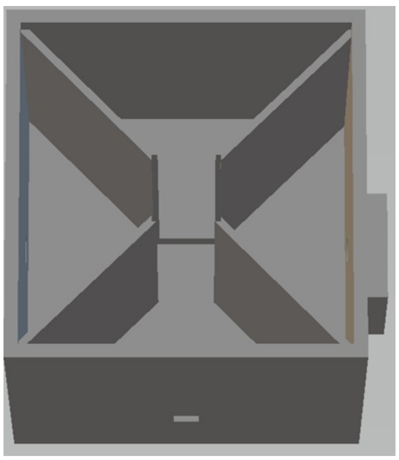

(a) Initial square design.

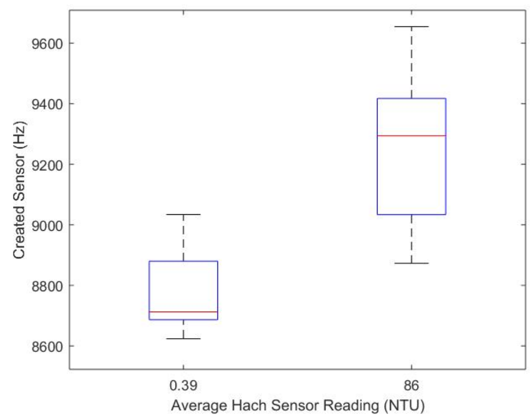

(b) Frequency output for initial square sample holder.

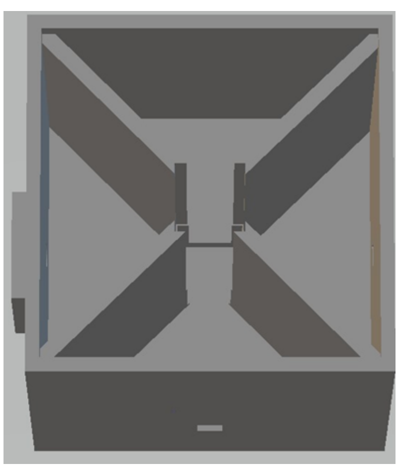

(c) Revised square sample holder with thicker walls and tighter fit to cuvette.

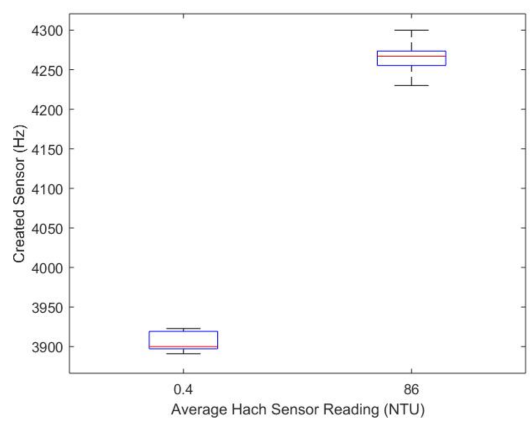

(d) Frequency output for revised square sample holder design.

Figure 6. Square cuvette sample holder designs with a light-to-frequency converter at 90° from the IR LED as well as the results from validation tests.

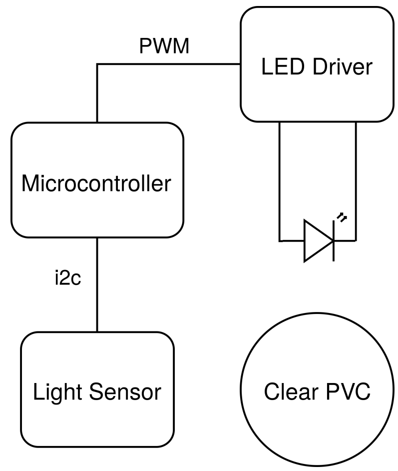

Figure 7. Low-cost continuous turbidity monitoring system diagram.

With these results, we conclude that a sample-based low-cost nephelometric turbidity sensor using a light to frequency converter can provide the minimum resolution required for water quality monitoring ($\approx$ 0.1 NTU). Our revised cuvette-based sample holder successfully reduced variation but would require further study to fully characterize the performance. This general design will be used to inform the development of a low-cost continuous turbidity sensor.

5. Low-Cost Continuous Turbidity Sensing

From our previous experiments, we have validated that a low-cost nephelometric turbidity sensor can meet the requirements (i.e., $\approx$ 0.1 NTU accuracy) needed for water quality monitoring applications. To provide continuous turbidity data, we will adapt the basic sensor design for flow-through applications. Many applications, such as drinking water and agriculture use commonly available pipes to transport water, such as PVC. In the U.S., schedule 40 and 80 are common specifications of PVC pipe which are available in a variety of colors and importantly for this application, clear.

Our approach to the continuous low-cost turbidity sensor is to attach an LED and a light sensor on the outside of a clear PVC pipe segment oriented 90° apart in the nephelometric configuration. In the previous tests, the separation between the LED and sensor was proportional to the width of the cuvette, which is 10 mm. In piped configuration, this distance will be proportional to the pipe size, which could be several inches. Because the LED will be illuminating a much larger volume of water, we surmise it is useful to increase the brightness. High powered IR LEDs (several watts) are not readily available and specialty IR LEDs are expensive. However, high-powered white LEDs are common. As a result, we replaced the IR LED with a commonly available Cree XLamp white LED (4000K). To properly drive the LED, we use a commonly used constant current LED driver (Diodes Incorporated AL8805) configured to deliver up to 500 mA of current to the LED via a PWM control signal. This allows us to also replace the IR light-to-frequency converter with a low-cost ambient light sensor (TSL4531). These sensors are commonly used to control display brightness and provide a digital i2c output of light intensity that is calibrated to Lux. To support wireless data collection, we connect the LED driver and light sensor to an ESP32 wifi-enabled microcontroller. A diagram of the complete low-cost continuous turbidity sensing system is shown in Figure 7.

To provide consistent contact with the PVC pipe, we designed a 3D-printable mounting ring to mechanically fix the LED and sensor to the pipe. Different pipe diameters can be accommodated by

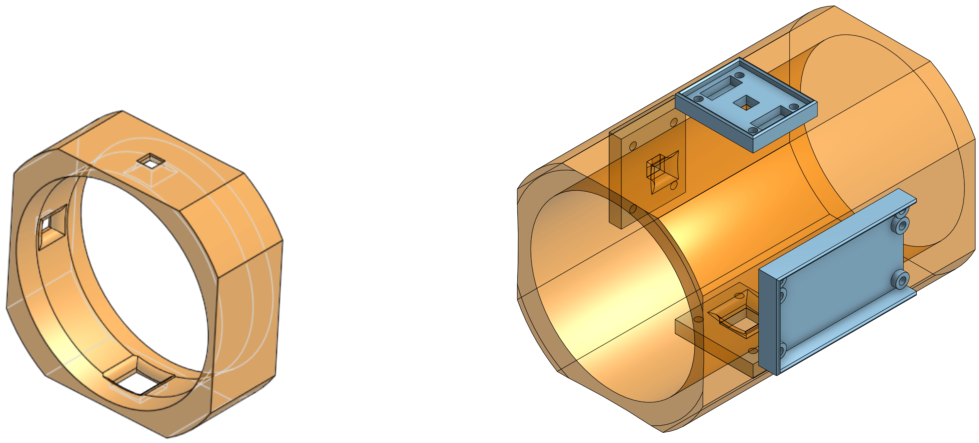

(a) Initial design. **(b)** Revised design including PCB mounts and reduced ambient light.

Figure 8. Nephelometric sensor mounts for clear pipes.

adjusting the dimensions of the mounting ring. Figure 8 shows a rendering of a) our initial design and b) revised mounting ring. With the initial design, the LED and ambient light detector were mounted to a small PCB and glued to the mounting ring. Because the PCB used through-hole connections, solder joins on the bottom of the PCB caused an uneven fit with the ring. This mechanical ring was also narrow (1 inch) and allowed ambient light to reach the light sensor. As a result, the design was revised to include PCB standoffs, recessed areas to accommodate solder joints, and the height of the ring was increased to block more ambient light. The part was sized to tightly fit over a section of 2-inch schedule 40 clear PVC pipe and printed in black ABS on an Ultimaker 2+ 3D printer. Black was selected to minimize reflected light in the sensor. Although we did not characterize this effect, we tested other colors and found black to have the lowest light level with the LED on. This suggests that reflections are minimized as desired.

5.1. Lab Calibration

Four sensors were constructed and tested over the range of 0 NTU to 100 NTU to explore the variation that exists in the different sensors made from the same components. The sensors are labeled with the last two digits of their ESP32 WiFi MAC address. For lab calibration, the sensors were oriented vertically over a short section of clear PCV pipe with silicone caulk securing the mounting ring to the pipe and a Qwik Cap sealing the bottom as shown in Figure 9. Test solutions were added to fill the PVC pipe and a cover was placed over the top to block ambient light. The sensor was allowed to run for 15 minutes before data was collected for analysis as the temperature of the components could have an effect on the sensor readings. The 15 minute run time was also used to allow any bubbles that formed when the sample was poured to dissipate. Each of the samples was tested in each sensor for 10 minutes while manual turbidity readings were made every 2 minutes using a Hach 2100P turbidity meter to see if the turbidity standards were changing. The created sensor read the light intensity at 90-degrees, 180-degrees and the dark reading (reading without the LED on) every 6 seconds during the sampling interval.

The samples were created using formazin standards by diluting a 4000 NTU formazin standard with deionized water ($\approx$ 0.20 NTU) to produce test solutions with values of (0.20, 5, 20, 40, and 100 NTU) [13]. The sensor was rinsed thoroughly with deionized water between different samples to clean any residual sample out of the pipe.

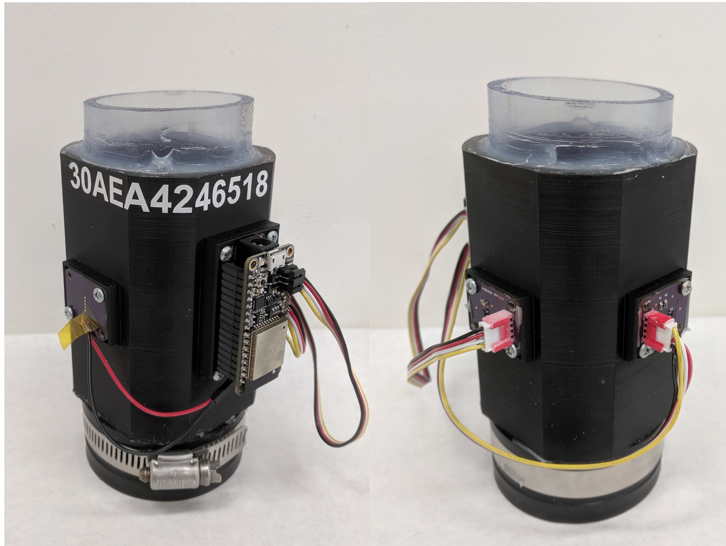

Figure 9. Sensor 18 configured for lab calibration.

Table 2. Individual and combined model parameters, R^2, root mean square error (RMSE), and error variance (σ^2) for using the 90 and 180 degree sensors, only the 90 degree, and only the 180 degree sensor respectively.

Device	Sensor(s)	c_1	c_2	c_3	ϵ	R^2	RMSE	σ^2
Sensor 8C	90, 180	0.0999	0.1952	-0.0017	6.9631	0.9997	0.2052	0.0421
Sensor 8C	90	0.1205	0.2118	0.0000	-14.9238	0.9997	0.2113	0.0447
Sensor 8C	180	0.2861	0.0000	-0.0215	262.0761	0.9970	0.6242	0.3896
Sensor 18	90, 180	-0.0905	0.1817	-0.0028	18.3600	0.9996	0.1309	0.0171
Sensor 18	90	-0.0829	0.2107	0.0000	-16.4420	0.9995	0.1442	0.0208
Sensor 18	180	-0.1424	0.0000	-0.0203	235.4548	0.9961	0.3991	0.1593
Sensor 94	90, 180	-0.4166	0.3302	0.0080	-123.8483	0.9994	0.3648	0.1330
Sensor 94	90	-0.3100	0.2329	0.0000	-16.3303	0.9991	0.4393	0.1930
Sensor 94	180	-0.0428	0.0000	-0.0192	240.2401	0.9962	0.9064	0.8216
Sensor B8	90, 180	-0.3393	0.2889	0.0030	-61.0751	0.9999	0.2060	0.0424
Sensor B8	90	-0.3335	0.2508	0.0000	-20.5734	0.9999	0.2318	0.0537
Sensor B8	180	-0.1870	0.0000	-0.0194	244.9908	0.9981	0.8297	0.6884
Combined	90, 180	0.4329	0.2303	-0.0001	-15.9821	0.9897	1.3933	1.9414
Combined	90	0.4367	0.2317	0.0000	-17.5408	0.9897	1.3941	1.9436
Combined	180	2.0732	0.0000	-0.0150	184.1420	0.7409	6.9825	48.7557

After the laboratory sampling was complete, the data for each sensor was fit to a model of the form:

$$NTU = c_1 \times d_0 + c_2 \times d_{90} + c_3 \times d_{180} + \epsilon$$

Where d_0 is the light intensity with the LED off in lux, d_{90} is the light intensity with the LED on at 90 degrees from the LED in lux, d_{180} is the light intensity with the LED on at 180 degrees from the LED in lux, and ϵ is the y-intercept. These values were computed using ordinary least squares linear regression comparing the predicted NTU to the most recent manual NTU reading of the sample. Models were generated for each sensor individually in addition to a combined model using data from all of the sensors. To explore the impact of each sensor (90 degrees and 180 degrees from the LED), models were

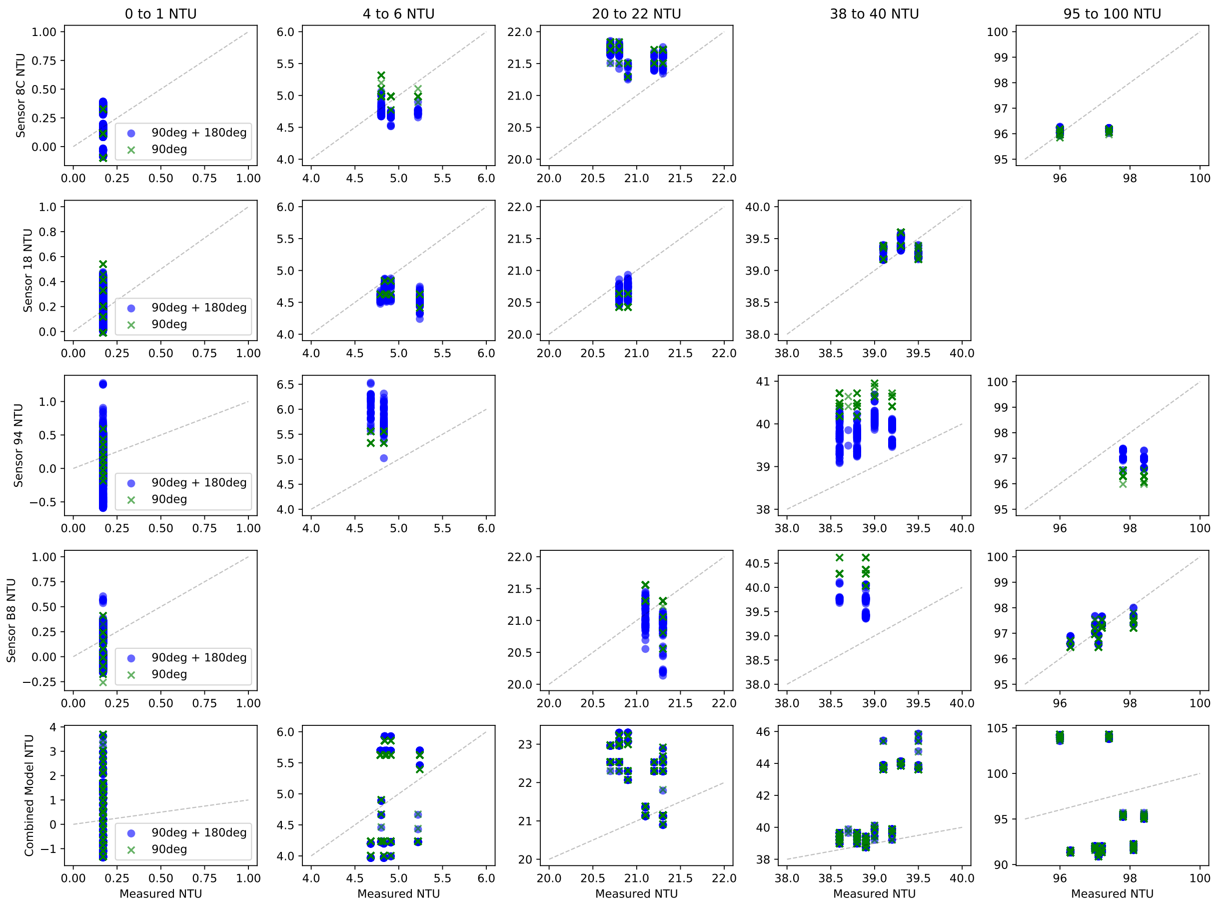

Figure 10. Measured NTU vs. computed NTU for the individual and combined models on 5 NTU ranges.

generated with each sensor individually as well as both of the sensors. Table 2 shows all computed model parameters, the R^2 measure, root mean square error (RMSE), and standard deviation (σ^2) of the error.

From these results, we see that the computed model fits the data well in all cases excepted for the combined model using only the 180-degree sensor. The device-specific models have the best fit, indicating some variation between sensors. To further explore this Figure 10 shows several plots of measured NTU vs. modeled NTU. The first four rows are the device-specific models and the last row is the combined model generated by fitting the model to all of the sensor data. The columns show increasing NTU ranges. Missing plots result from not testing every turbidity sample on every sensor. The results with only the 180-degree sensor are omitted for clarity as this case performed significantly worse than the others.

Figure 11 shows the error distribution using the computed models. The individual model error is computed individually across all device specific models and combined to create a single plot. We can see that the individual device models perform better than the combined models and there is a small affect of using both 180 and 90-degree sensors with the device-specific models. Using both sensors produced a wider error distribution at low NTU and smaller error distribution at higher NTU, however, the median error as smaller in every range except 4 to 6 NTU. For the combined model, the 180-degree sensors do not improve the results.

These results show the using readings directly from the sensor will not achieve our goal of 0.1 NTU accuracy. However, because the median values have less than 0.1 NTU error, averaging multiple samples

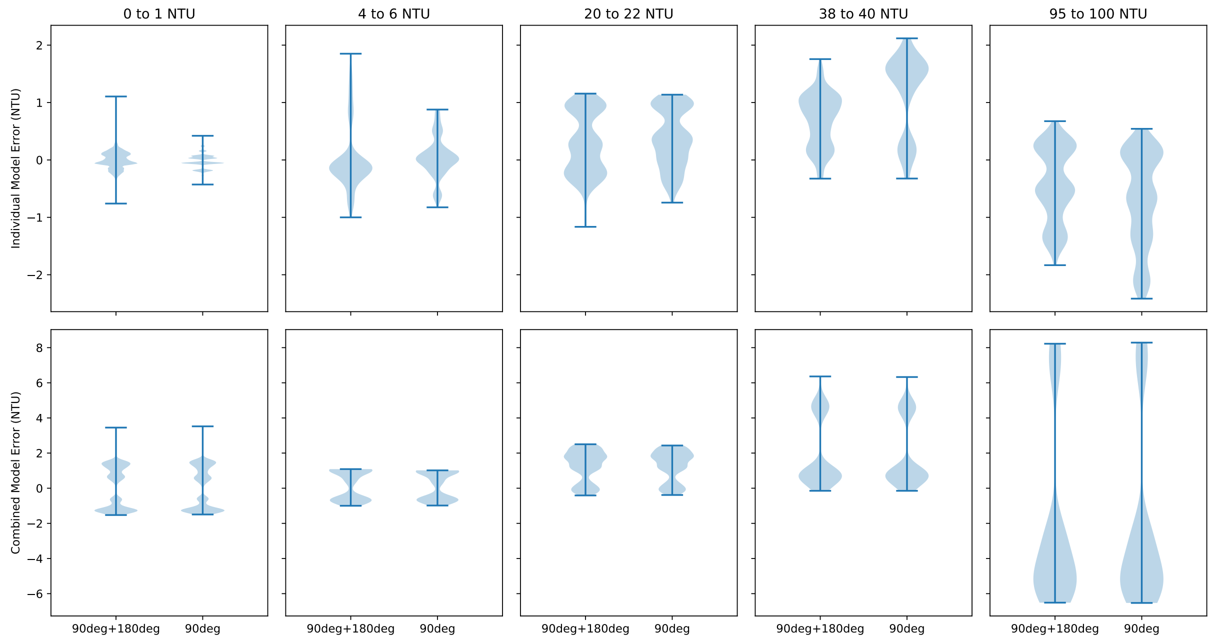

Figure 11. Distribution of error the individual models and the combined model on the 5 NTU ranges measured.

could reduce this noise to approach the accuracy goal. This dataset did not have enough samples to fully investigate this question, so we will explore this in the next section.

5.2. Pumped Tank Test

Having calibrated and explored the performance of the low-cost continuous turbidity sensor in a laboratory setting, we now move to a simulated real-world test. For this test, we used a 1,000-gallon water tank and a 1,000 GPH pool pump without a filter to circulate the water. To explore if the sensor should be on the pump inlet or outlet, we installed a sensor on both. Sensor B8 was installed on the pump inlet and Sensor 94 was installed on the pump outlet.

The tank was filled with fresh drinking-quality water and manual turbidity measurements were made daily with the Hatch 2100P turbidimeter. These measurements were linearly interpolated between samples to produce a continuous turbidity value in the tank for analysis. The low-cost continuous sensor readings were made once every 6 seconds. Timestamps for each sample were recorded by the sensor and the clock was synchronized with a public NTP server at the start of the experiment. The timestamp and raw sensor values were then transmitted over a WiFi network to a database for storage. For analysis, the raw sensor values were linearly interpolated to a constant 1 Hz rate and a 20-minute moving average of 1,200 samples at 1 Hz containing about 200 raw samples was computed over 5-minute periods, resulting in 288 samples per day. We chose these values to reduce the amount of data as we expect turbidity to change relatively slowly and simultaneously reduce sensor noise by averaging multiple readings. Experimentally we found that averaging over 1-minute periods (10 raw samples) was sufficient to eliminate the majority of the sensor noise but we elected to use longer periods in our analysis to produce the desired sample rate.

The filtered sensor readings were then used in the device-specific lab models (Table 2) to estimate the NTU reading in the tank. A small offset was present at installation, so we adjusted each individual model's ϵ parameter after making the first manual reading to remove this error. Shortly after the installation,

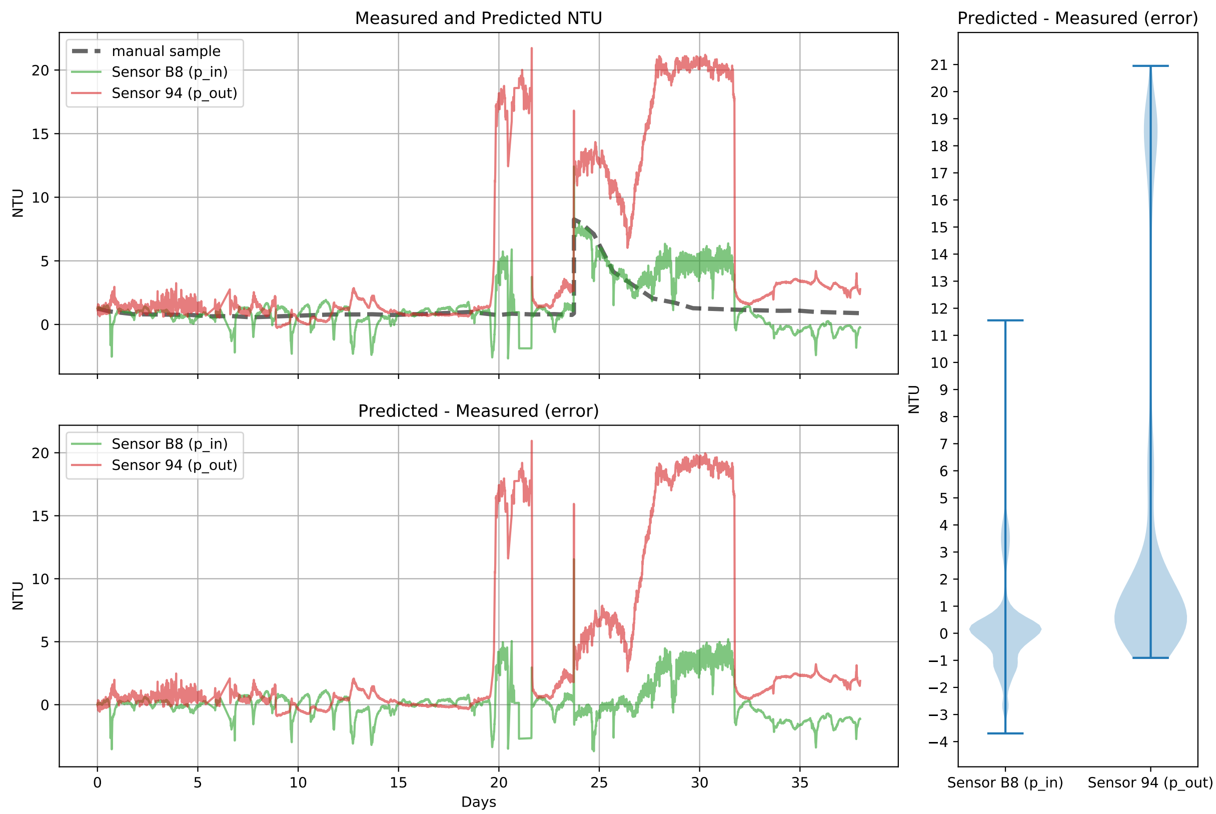

Figure 12. Pumped tank continuous turbidity measurements from the pump inlet (p_in) and outlet (p_out) sensors vs. manual samples.

Sensor 94 failed and the LED and light sensor was replaced with the components from Sensor 18. Data is reported as Sensor 94, however, the model generated by Sensor 18 is used to estimate NTU. Figure 12 shows results for thirty-eight days of measurements. During two intervals between days 5 and 7, the data collection failed and no samples were recorded. For analysis, the missing data were linearly interpolated between the available samples.

Initially, through day 5, the sensor on the outlet has significant noise. On day 6 we discovered that bubbles were present in the pipes near the outlet sensor and we purged the air from the pipes. On day 9 we discovered that a small hole was allowing air into the pipes. We sealed the hole and both sensors showed significantly reduced noise after this. In sealing the hole, we repositioned the outlet sensor, which caused an offset in the readings. At day 20 there was another air leak that caused significant error and was sealed by day 22.

To investigate the response of the sensor to changing turbidity, we continued our measurements and added one-quarter cup of Coffee mate® powdered coffee creamer to the 1,000-gallon tank on day 23 at the pump inlet. This quickly increased the tank turbidity to about 8 NTU. The inlet sensor closely tracked this change demonstrating the impulse response of the sensor. On day 27 both sensors NTU reading begin increasing and we discovered the patch to the pipe had failed. We let this continue until day 32 when it was patched again.

Overall the inlet sensor was less sensitive to the bubbles but showed a strong daily pattern of large negative NTU spikes in the late morning to early afternoon. This is almost certainly caused by increased ambient light hitting the sensor and water pipes. The pipes used were translucent and the inlet pipe was exposed to direct sunlight in the mornings. Because our lab experiments were taken in relatively dark conditions, the model did not account for the influence of ambient light. The overall error distribution for both sensors is also shown. The median error and standard deviation for the inlet and outlet sensors over the entire test were 0.0574, 1.482 NTU and 0.949, 6.417 NTU respectively.

5.3. Discussion

In this section, we describe the creation of a low-cost continuous nephelometric turbidity monitor built using commonly available components. The turbidity monitor is designed to fit over a short section of clear PVC pipe. This approach reduces the mechanical complexity of the system since no components are ever in direct contact with water.

Lab experiments demonstrated the median error was less than 0.1 NTU with some noise present in the readings. Averaging multiple readings can approach our goal of 0.1 NTU measurement accuracy under well-controlled conditions.

The pumped tank test demonstrated that the sensor can continuously measure turbidity installed either on the inlet and outlet of a pump. However, the inlet sensor had better impulse response to a turbidity change and was less susceptible to interference from bubbles. The inlet sensor showed more interference from ambient light but we attribute this to sensor positioning and not an artifact of the pump inlet. Neither sensor achieved the desired accuracy of better than 0.1 NTU over a long period, however, by eliminating ambient light and bubbles we believe performance can be significantly improved. Furthermore, even at the current level of performance, many applications could benefit from low-cost continuous turbidity monitoring by detecting larger changes in turbidity (e.g., > 1 NTU). Results from the last days of the experiment showed a significant offset was present suggesting that periodic calibration may be required. We plan to explore long-term stability in future work.

6. Conclusion and Future Work

In this paper, we explored the development of a low-cost continuous turbidity monitor. We started with readily available appliance sensors. While inexpensive, in our tests they do not have the required accuracy for water quality applications. They were also prone to a large amount of noise and are difficult to precisely calibrate. Examining prior work on low-cost turbidity sensors, we verified that accurate low-cost sample-based turbidity sensors can be constructed. In our tests, the main source of error was the imprecision of the sample holder (Cuvette or Test Tube) in the sensor apparatus. Using this design as a starting point, we adapted the sensor for use in piped-water applications. Lab tests verified that with individual calibration, accuracy better than 0.1 NTU is possible. A thirty-eight-day long experiment was performed with the constructed sensor in a piped-water application. The sensor showed more error than in the lab experiments, yielding ≈ 1 NTU accuracy and good response to changes in turbidity. The primary source of error was attributed to bubbles in the liquid and ambient light. This may be sufficient for some continuous monitoring applications. For other applications where higher accuracy is needed, we believe that by reducing ambient light on the sensor and eliminating all air from in the pipes will yield improved accuracy. Like all other turbidity sensors, periodic calibration is necessary to maintain the accuracy of the sensor.

As we found that device-specific calibration significantly improves performance, a simpler way to calibrate the sensor is recommended as lab-made turbidity standards are not commonly available by citizen scientists. There are other liquids that have consistent turbidity such as apple juice and tea which could be used for calibration. A validated procedure to calibrate the sensor with these liquids could be developed. We also plan longer trials to verify the long-term behavior of the sensor. One long-term concern is if and when to remove and clean the clear PVC section. Since PVC can develop a static charge, contaminants may be attracted to the sensor. It is not clear if the pumped liquid is sufficient to avoid these contaminants. We plan to redesign the sensor housing to simplify removal for inspection and cleaning.

1. United Nations Educational, Scientific and Cultural Organization (UNESCO). Water in the post-2015 development agenda and sustainable development goals, Discussion paper for the 21th session of the Intergovernmental Council of the International Hydrological Programme of UNESCO, 2014.
2. Burke, D.G.; Allenby, J. Low Cost Water Quality Monitoring Needs Assessment, 2013. accessed Feb 2019.
3. Metzger, M.; Konrad, A.; Blendinger, F.; Modler, A.; Meixner, A.; Bucher, V.; Brecht, M. Low-Cost GRIN-Lens-Based Nephelometric Turbidity Sensing in the Range of 0.1–1000 NTU. *Sensors* **2018**, *18*, 1115. doi:10.3390/s18041115.
4. Creative Uses of Custom Electronics for Environmental Monitoring at the Christina River Basin CZO. American Geophysical Union Annual Fall Meeting, San Francisco, CA, 2012.
5. Kelley, C.; Krolick, A.; Brunner, L.; Burklund, A.; Kahn, D.; Ball, W.; Weber-Shirk, M. An Affordable Open-Source Turbidimeter. *Sensors* **2014**, *14*, 7142–7155. doi:10.3390/s140407142.
6. Lambrou, T.P.; Panayiotou, C.G.; Anastasiou, C.C. A low-cost system for real time monitoring and assessment of potable water quality at consumer sites. SENSORS, 2012 IEEE. IEEE, 2012, pp. 1–4.
7. O'Dell, J.W. Method 180.1 Determination of Turbidity by Nephelometry. Environmental Monitoring Systems Laboratory Office of Research and Development U.S. Environmental Protection Agency, 1993.
8. Fondriest Environmental, Inc.. Fundamentals of Environmental Measurements: Measuring Turbidity, TSS, and Water Clarity, 2014. accessed 24-May-2018.
9. Amphenol. *TST-10 Turbidity Sensor Datasheet*, 2014.
10. GE Measurement & Control. *TSD-10 Turbidity Sensor Datasheet*, 2013.
11. Amphenol. *TSW-10 Turbidity Sensor Datasheet*, 2014.
12. Stoffregen, P. FreqCount Library. https://github.com/PaulStoffregen/FreqCount. [Version 1.3, Accessed 5/31/2018].
13. Sadar, M. Turbidity Standards. Technical Information Series – Booklet No. 12.